

Equilibrium and Kinetic Studies on Reactive Dye Adsorption Using Palm Shell Powder (An Agrowaste) and Chitosan

G. Sreelatha,[†] V. Ageetha,[‡] J. Parmar,[‡] and P. Padmaja^{*‡}

Department of Chemistry, Faculty of Science, The Maharaja Sayajirao University of Baroda, Vadodara, India, and Department of Applied Chemistry, Faculty of Technology & Engineering, The Maharaja Sayajirao University of Baroda, Vadodara, India

The adsorption of reactive dyes onto acid-treated palm shell powder (APSP) and chitosan has been investigated. The parameters affecting the rate process involved in the removal of dye like contact time, temperature, pH, adsorbent dose, and dye concentration were studied. pH 4 was suitable for the adsorption of both reactive dyes onto chitosan and was independent of pH in the range pH 2 to 9 using APSP as the adsorbent. The process of dye removal followed pseudosecond-order kinetics. The adsorption equilibria isotherms were analyzed by the Langmuir and Freundlich isotherms. The adsorption capacities were found to be 13.95 mg·g⁻¹ and 24.86 mg·g⁻¹ for reactive red 141 and reactive blue 21 using APSP as adsorbent. The adsorption capacities were found to be 22.48 mg·g⁻¹ and 70.08 mg·g⁻¹ for reactive red and reactive blue, respectively, using chitosan as the adsorbent.

Introduction

Dyes have been widely used including in the textile, paper printing, leather, color photography, and consumable industries. Reactive dyes are widely used because of their bright colors. Reactive dyes in wastewaters have limited biodegradability in an aerobic environment, and many azo dyes under anaerobic conditions decompose into potential carcinogenic aromatic amines. Most reactive dyes are stable to light and to biological degradation.¹

The conventional methods for the treatment of dye-containing wastewaters are coagulation and flocculation,² reverse osmosis,³ and activated carbon adsorption.⁴ These technologies do not show significant effectiveness or economic advantage. Despite the prolific use of activated carbon for wastewater treatment, carbon adsorption is considered as an expensive process, and this fact has prompted growing interest into the production of low cost alternatives to activated carbons in recent years.

A number of nonconventional, low-cost adsorbents have been used for the removal of dyes.^{5–20} However, an effort is being made to prepare better low-cost adsorbents as alternatives to activated carbon.

Palm fruit is available throughout coastal India. The shell of the palm fruit is thrown away when the fruit is eaten. Chitosan is a polysaccharide and has reactive properties, which can produce a number of derivatives having a wide range of uses.^{21–26} Chitosan carries a large number of amine groups on its chain and thus forms multiple complexes. At an acidic pH, it forms complexes with polyanions and complexes with colorants and heavy metals.²⁷

An effort has been made to explore the use of palm shells after powdering and carbonizing with sulfuric acid as a low-cost adsorbent. The present study involves the use of chitosan and acid-activated palm shell powder for the removal of acidic

reactive dyes reactive blue 21 (RB-21) and reactive red 141 (RB-141). The equilibrium isotherm and kinetic characteristics of reactive dye adsorption on the above-mentioned adsorbents were investigated using bench scale batch tests. A comparison of the adsorption capacities with other adsorbents reported in the literature is given in Table 1.

Materials and Methods

Preparation of Adsorbent. Palm shells obtained from the coastal areas of Andhra Pradesh were washed, sun-dried for 24 h, and ground using a jaw crusher. They were then dried at 110 °C, and the cleaned powder was mixed with concentrated H₂SO₄ (sp. gr. 1.84) in a 1:1.5 weight ratio and allowed to stand in an oven maintained at (140 to 160) °C for 24 h. The resulting char was thoroughly washed with water followed by a 2 % solution of NaHCO₃ until effervescence ceased and then was left to soak in a 2 % solution of NaHCO₃ overnight. The acid-treated palm shell powder (APSP) was then separated, washed with water until it was free of bicarbonate, and dried at 105 °C. Chitosan flakes (87.6 % deacetylated and molecular weight 5.5·10⁵ g/mol) were from Sigma. The Chitosan flakes were used for further experimental studies as an adsorbent.

Preparation of Dye Solutions. Stock solutions of dyes (1 g·L⁻¹) were prepared by dissolving accurately weighed amounts of RB-21 and RR-141 in double-distilled water with subsequent dilution to the required concentration. The structure of the dyes used in this study are given in Table 2.

Sorption Procedure. A 10 mg·L⁻¹ solution of RR-141 and RB-21 was prepared and scanned in the range of (400 to 800) nm using a SYSTRONICS Digital 166 model visible spectrophotometer. The wavelength that provided maximum absorbance was determined, and a calibration was prepared to determine the concentration of each dye after adsorption of the dye on APSP in further experiments. The dye concentration in the filtrate was determined by measuring the absorbance at the wavelength of maximum absorption at (648 and 540) nm for RB-21 and RR-141, respectively. The percentage removal of

* Corresponding author. Tel.: +91-265-2795552; Fax: +91-265-2795552; E-mail address: p_padmaja2001@yahoo.com (P. Padmaja).

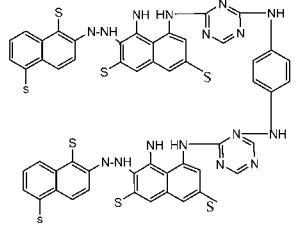
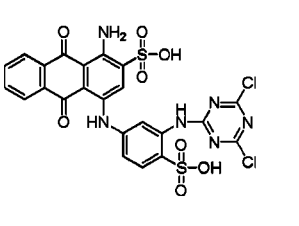
[†] Department of Applied Chemistry, Faculty of Technology & Engineering.

[‡] Department of Chemistry, Faculty of Science.

Table 1. Comparison of Adsorption Capacities of Agro-Based Adsorbents

adsorbent	dye	adsorption capacity	reference
activated carbon from coir pith	Congo red	6.7 mg·g ⁻¹	30
carbon slurry waste	Congo red	272 mg·g ⁻¹	35
sun flower stalk	Congo red	26.8 mg·g ⁻¹	17
waste metal hydroxide sludge	reactive red 2, reactive red 120, and reactive red 141	(48 to 62) mg·g ⁻¹	36
preprotonated chitosan	reactive black 5	(750 to 1000) mg·g ⁻¹	37
commercial activated carbon	reactive orange	714 mg·g ⁻¹	38
ethylenediamine modified rice hull	reactive orange 16	24.88 mg·g ⁻¹	39
surfactant-modified activated carbon	reactive black 5	0.11 mmol·g ⁻¹	40
APSP, chitosan	reactive red	(13.94 and 22.48) mg·g ⁻¹	present study
APSP, chitosan	reactive blue	(22.48 and 70.02) mg·g ⁻¹	present study

Table 2. Structure of Dyes

Dyes	Reactive red - 141	Reactive blue - 21
Structural Formula		

the dye and the amount adsorbed (mg·g⁻¹) were calculated by the following relationship:

$$q_e = (C_i - C_e)/m$$

where C_i is the initial concentration of the dye in mg·L⁻¹; C_e is the equilibrium concentration of dye in mg·L⁻¹; m is the mass of adsorbent in g·L⁻¹; q_e is the amount of dye adsorbed per gram of adsorbent. The experiments done without adsorbent were treated as blanks, and they showed no precipitation of dye occurred under the conditions selected.

Adsorption Isotherms. The results of the adsorption experiments were analyzed using the Freundlich and Langmuir isotherm models to determine the mechanistic parameters associated with the adsorption. The linearized Freundlich isotherm is:

$$\log q_e = \log K_F + 1/n \log C_e \quad (1)$$

where q_e = amount of solute adsorbed per unit weight of adsorbent (mg·g⁻¹), C_e = concentration of solute remaining in solution at equilibrium (mg·L⁻¹), and K_F and n are the Freundlich constants.

The Langmuir isotherm model used is given as:

$$q_e = (q_m K_a C_e)/(1 + K_a C_e) \quad (2)$$

where q_m = amount of solute adsorbed per unit weight of adsorbent in forming a complete monolayer on the surface (mg·L⁻¹) and K_a = a constant related to the energy or net enthalpy.

Adsorption Dynamics. The kinetics of sorption of anionic dyes was investigated using the pseudofirst-order, pseudosecond-order, and intraparticle diffusion reaction models. The pseudofirst order is given by:

$$\log(q_e - q_t) = \log q_e - K_1 t/2.303 \quad (3)$$

where q_e and q_t are the adsorption capacity at equilibrium and at time t , respectively (mg·g⁻¹); K_1 is the rate constant of pseudofirst-order adsorption (L·min⁻¹). K_1 and q_e can be determined from the slope and intercept of the plot, respectively.

The pseudosecond-order reaction kinetic model is expressed as:

$$t/qt = 1/(K_2 q_e^2) + t/q_e \quad (4)$$

where K_2 is the rate constant of pseudosecond-order adsorption (g·mg⁻¹·min⁻¹), which is the integrated rate law for a pseudosecond-order reaction.²⁸

The equation for the Weber Morris intraparticle diffusion model is

$$q_t = K_i t^{0.5} \quad (5)$$

where k_i is the intraparticle diffusion rate constant (mg·g⁻¹·min⁻¹).

Fourier Transform Infrared Spectroscopy (FTIR). FTIR was used to determine the vibrational frequencies of the functional groups in the adsorbents. The spectra were collected by a Perkin-Elmer RX1 model within the wavenumber range of (400 to 4000) cm⁻¹. Specimens of samples were first mixed with KBr and then ground in an agate mortar at an appropriate ratio of 1/100 for the preparation of the pellets. The resulting mixture was pressed at 10 tons for 5 min. Sixteen scans and an 8 cm⁻¹ resolution were applied in recording the spectra. The background obtained from the scan of pure KBr was automatically subtracted from the sample spectra.

Scanning Electron Microscopy (SEM). A topography analysis of certain features was visualized by using a SEM microscope (JEOL, model JSM-5610LV). Samples were mounted onto metal holders using a conducting substrate. The SEM analysis enables the direct observation of the changes in the surface microstructures of the adsorbents that are due to the chemical surface modifications and the elemental composition.

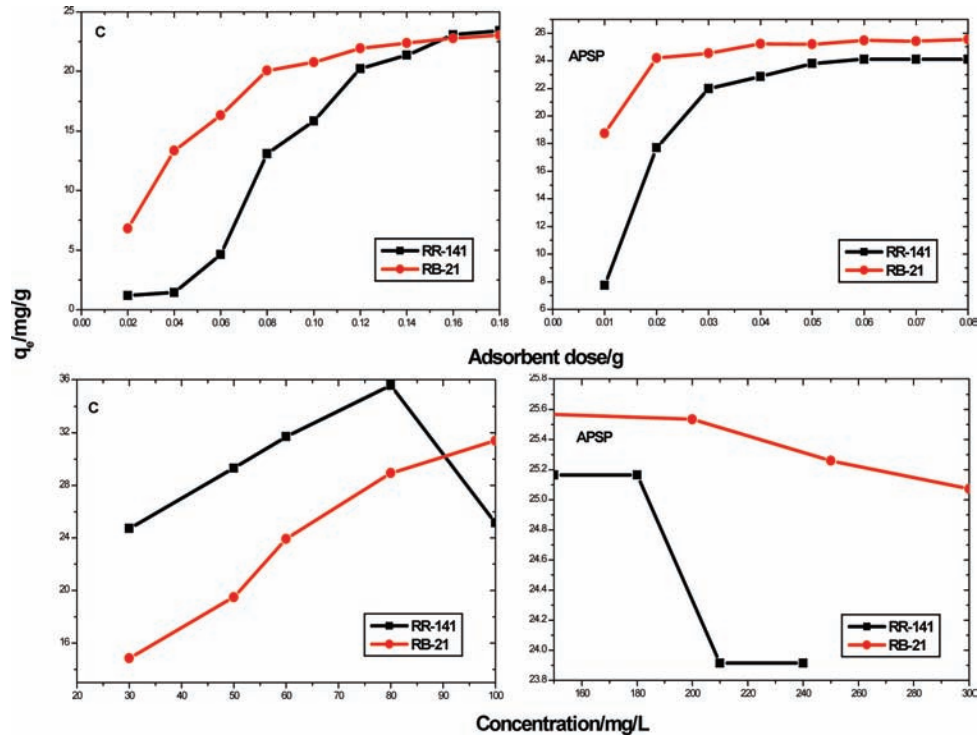


Figure 1. Effect of adsorbent dose and concentration on the amount of dye adsorbed on APSP and chitosan.

Results and Discussion

Effect of Adsorbent Dose. The effect of the amount of APSP and chitosan on the uptake of RR-141 and RB-21 was studied, and the results have been presented in Figure 1. The experiments were conducted by taking different adsorbent doses from (0.01 to 0.2) g in 25 mL of dye solution. Other parameters like pH, contact time, and temperature were kept constant. The removal increased from 74 % to 100 % and 30 % to 96 % for RB-21 and for RR-141, respectively, with an increased adsorbent dose from (0.01 to 0.08) g in the case of APSP and from 27 % to 92

% and 4 % to 94 % for RB-21 and RR-141, respectively, with an increased adsorbent dose from (0.02 to 0.18) g in the case of chitosan as the adsorbent. This can be attributed to the larger availability of active sites for the same number of adsorbate molecules. The dyes are seen to require a greater dose of chitosan as compared to palm shell powder which could be attributed to a lesser number of active sites as compared to APSP.

Effect of Contact Time. To evaluate the effect of contact time between dyes and sorbent (APSP and chitosan), the

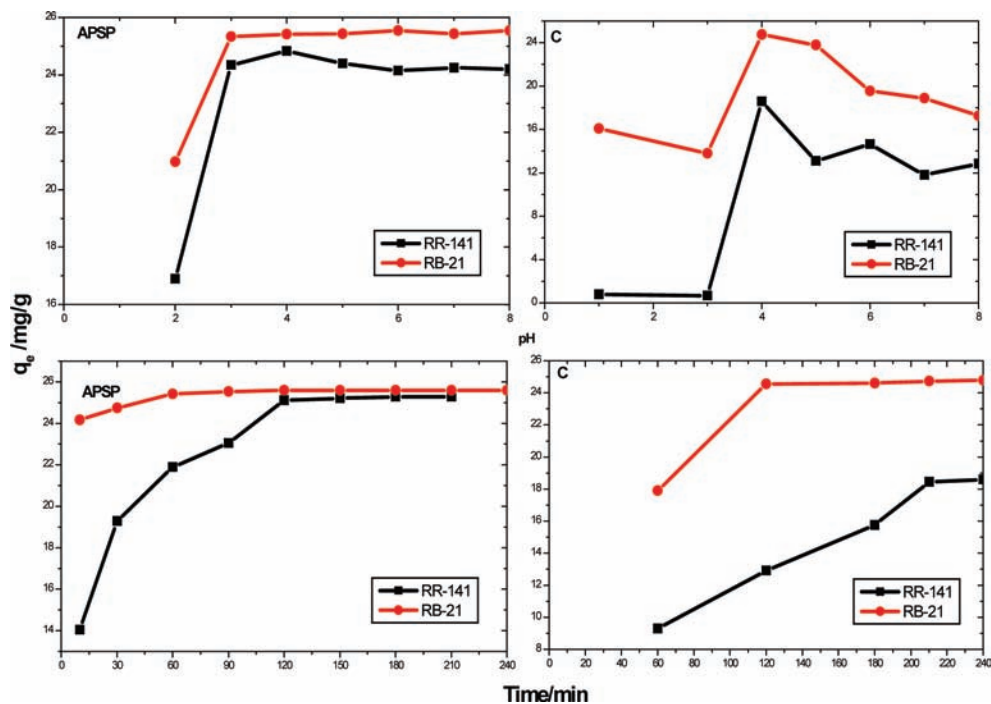


Figure 2. Effect of pH and time on the amount of dye adsorbed on APSP and chitosan.

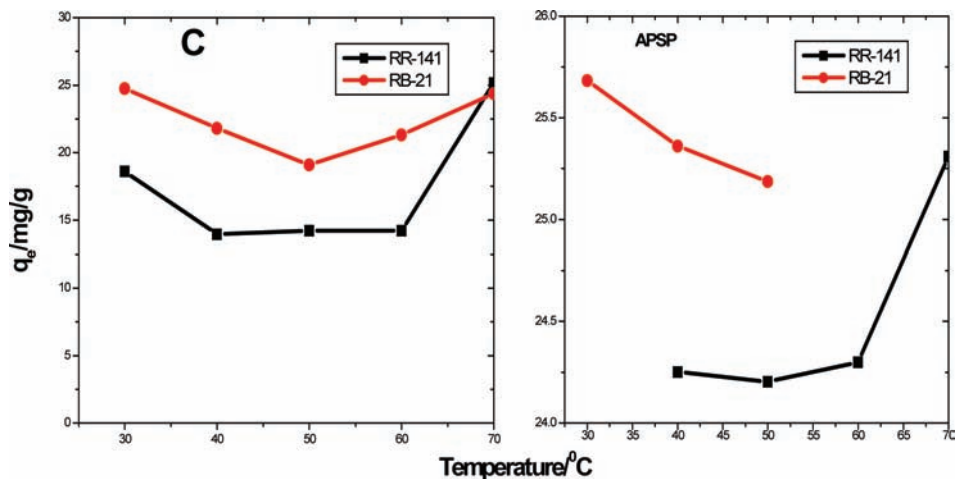


Figure 3. Effect of temperature on the amount of dye adsorbed on APSP and chitosan.

agitation time was varied between (60 and 240) min for chitosan and (10 and 120) min for APSP. The results are shown in Figure 2. It is seen that sorption is fast and equilibrium is achieved within 60 min for APSP and ~ 120 min for chitosan. Chitosan requires a greater contact time to achieve equilibrium.

The sorption of dyes was rapid during the initial stages of the sorption process, followed by a gradual process. The dye molecules have to first encounter the boundary layer effect and then adsorb from the surface, and finally they have to diffuse into the porous structure of the adsorbent which takes a longer time.²⁹

Effect of Reactive Dye Concentration. The effect of reactive dye concentration on their uptake by APSP and chitosan were studied at constant temperature for each of the dyes. The results in Figure 1 indicate that the increase in reactive dye concentration increases the uptake of both dyes in the case of both APSP and chitosan.

Effect of pH. The effect of initial pH on the sorption process was investigated. The effect of pH on the adsorption of RB-21 and RR-141 by chitosan and APSP was studied by varying the solution pH over a range of 1 to 11 using 0.1 N NaOH/HCl. The results in Figure 2 indicate that when APSP was used as adsorbent the removal was at a maximum at the initial pH of 3 and 4 for RB-21 and RR-141, respectively, and remained constant with (97 to 100) % removal up to pH 9.0. This suggests that two possible mechanisms of the adsorption of reactive dyes on APSP may be operating. At acidic pH an electrostatic attraction exists between the protonated surface of APSP and the negatively charged acidic dyes. The removal of anionic dyes at alkaline pH where the adsorbent is negatively charged cannot be explained based on electrostatic attraction. There might be another mechanism of adsorption like ion exchange or chemisorption which might be operative. A similar trend was observed for the adsorption of Congo red on activated carbon prepared

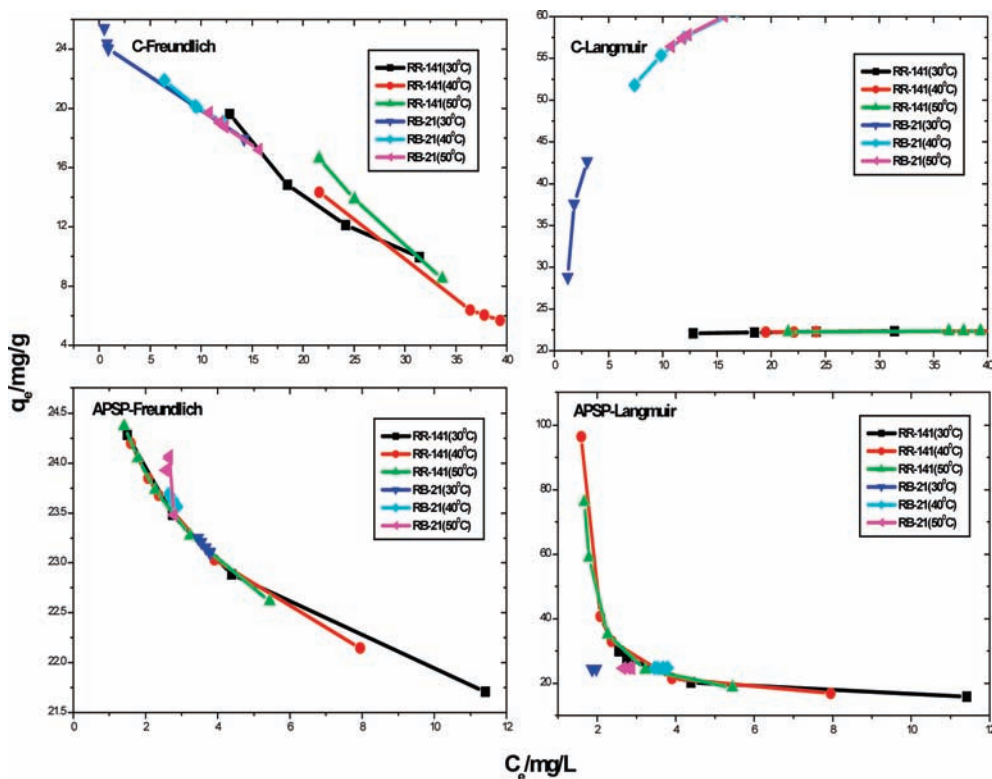


Figure 4. Isotherm for RR-141 and RB-21.

Table 3. Isotherm Parameters

isotherms	parameters	APSP		chitosan	
		RR-141	RB-21	RR-141	RB-21
Freundlich			30 °C		
	$K_f / (\text{mg} \cdot \text{g}^{-1}) \cdot (\text{dm}^3/\text{mg})^{1/n}$	24.8307	25.3472	24.2141	24.732
	N	-18.14	-11.99	-0.483	-9.5474
	R^2	0.949	0.938	0.963	0.912
			40 °C		
	$K_f / (\text{mg} \cdot \text{g}^{-1}) \cdot (\text{dm}^3/\text{mg})^{1/n}$	25.547	25.260	28.1916	24.732
	N	-11.32	-14.934	-11.341	-20.012
	R^2	0.931	0.9406	0.897	0.925
			50 °C		
$K_f / (\text{mg} \cdot \text{g}^{-1}) \cdot (\text{dm}^3/\text{mg})^{1/n}$	28.6767	25.5517	24.991	22.991	
N	-6.29842	-20.3046	1	8.417	
R^2	0.966309	0.958	1	0.938	
Langmuir			30 °C		
	q_e (exp)	19.2940	23.574	18.6035	19.082
	$q_m / \text{mg} \cdot \text{g}^{-1}$	7.713	19.040	5.0499	16.548
	$K_d / \text{L} \cdot \text{mg}^{-1}$	-0.392	11.99	-0.0738	-0.611
	R^2	0.95	0.976	0.916	0.967
			40 °C		
	q_e (exp)	22.809	25.360	13.9428	17.896
	$q_m / \text{mg} \cdot \text{g}^{-1}$	18.62	13.167	19.157	22.391
	$K_d / \text{L} \cdot \text{mg}^{-1}$	-2.021	16.432	-4.788	-8.474
	R^2	0.937	0.997	0.912	0.997
			50 °C		
	$q_m / \text{mg} \cdot \text{g}^{-1}$	13.954	24.866	22.480	70.028
$K_d / \text{L} \cdot \text{mg}^{-1}$	-0.73354	34.079	4.455	0.384	
R^2	0.974	0.9998	0.921	0.977	

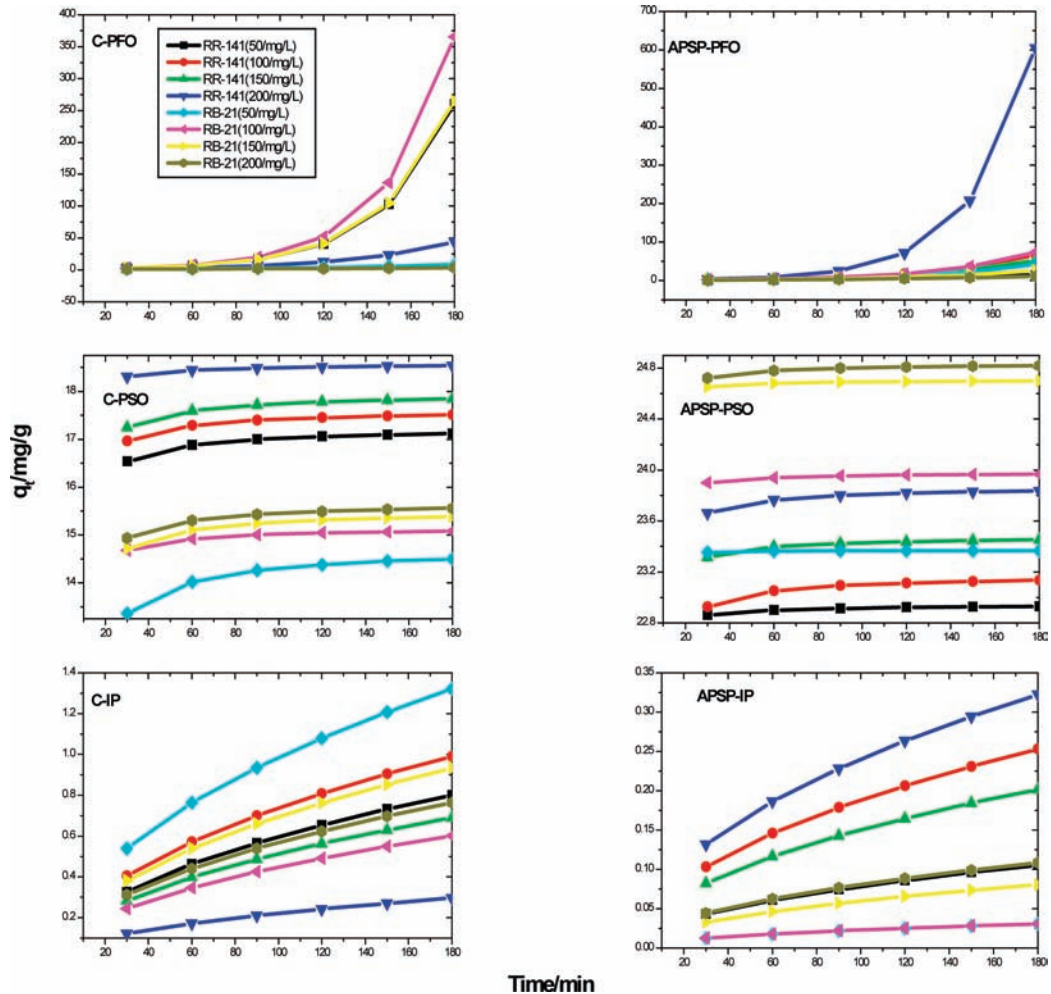


Figure 5. Kinetic models for RR-141 and RB-21.

Table 4. Kinetic Parameters

kinetics	parameters	APSP		chitosan					
		RR-141	RB-21	RR-141	RB-21				
pseudo 1 st order (PFO)	$q_e/\text{mg}\cdot\text{g}^{-1}$ K/min^{-1} R^2	12.442 0.0213 0.983	50 $\text{mg}\cdot\text{L}^{-1}$		17.416 9.8798 0.990	28.707 0.0330 0.813			
			0.3763 0.0234 0.944	100 $\text{mg}\cdot\text{L}^{-1}$			1.2159 0.0149 0.9473	13.77 0.0430 0.9536	
				0.2160 0.0234 0.9621					150 $\text{mg}\cdot\text{L}^{-1}$
	0.5275 0.0358 0.9307	200 $\text{mg}\cdot\text{L}^{-1}$			1.5023 0.0309 0.9473	1.064 0.0146 0.978			
		26.917 0.0371 0.9964	50 $\text{mg}\cdot\text{L}^{-1}$				27.956 2.750308×10^{-4} 0.980	27.948 1.3352642×10^{-3} 0.990	
			23.172 0.1568 0.986	100 $\text{mg}\cdot\text{L}^{-1}$					17.96 0.0442 0.998
	23.479 0.202 0.985			150 $\text{mg}\cdot\text{L}^{-1}$		17.62 0.0483 0.999			
		23.870 0.15681 0.984		200 $\text{mg}\cdot\text{L}^{-1}$			17.23 0.0456 0.999	14.75 0.0217 0.985	
			1.35402 0.1899	50 $\text{mg}\cdot\text{L}^{-1}$					1.1926 0.999
	0.01504 0.952			100 $\text{mg}\cdot\text{L}^{-1}$		0.05144 0.967			
		0.01805 0.9788		150 $\text{mg}\cdot\text{L}^{-1}$			0.0567 0.926	0.0448 0.9617	
			0.00786 0.9170	200 $\text{mg}\cdot\text{L}^{-1}$					0.056 0.960

from coir pith,³⁰ adsorption of Congo red,¹⁰ acid brilliant blue,¹³ and acid violet¹⁴ on a biogas residual slurry and adsorption of Congo red on waste orange peel²⁰ and banana pith.¹⁶

Figure 2 represents the RB-21 and RR-141 removal efficiency at equilibrium for varying pH in the range of 1 to 10 using chitosan as an adsorbent. The optimum pH is 4 for both RB-21 and RR-141 using chitosan. When the pH is lower than the $\text{p}K_a$ of chitosan, the nitrogen-containing functional groups of chitosan are protonated, and the positive charge would be expected to attract anions. At neutral pH the electrostatic balance between anionic and cationic groups on chitosan would make it less favorable for dye binding.

Effect of Temperature. The removal of RR-141 and RB-21 was investigated as a function of temperature, and results are given in Figure 3. The removal increased from 77 % to 100 % and 93 % to 100 %, respectively, using APSP as adsorbent by increasing the temperature from (30 to 70) °C, and 37 % to 100 %, and 66 % to 97 %, respectively, using chitosan as adsorbent. The extent of adsorption of both dyes using both of

the adsorbents was found to increase with temperature, indicating the endothermic nature of the process. The increase in dye adsorption with increasing temperature might be due to an increase in the number of active surfaces available for adsorption with an increase in temperature and due to an enhanced rate of intraparticle diffusion of the adsorbate, as diffusion is an endothermic process.³¹

Adsorption Isotherms. The adsorption isotherms were obtained for RB-21 and RR-141 onto chitosan and APSP adsorbent systems (see Figure 4). The Langmuir and Freundlich isotherm constants at different temperatures for the adsorption of RR-141 and RB-21 onto chitosan and APSP are reported in Table 3. Equilibrium sorption data of RR-141 and RB-21 onto APSP and chitosan fitted both the Langmuir and Freundlich equations. Similar observations were made by Sarkar et al.^{32–34} Comparing the parameters K_f and q_m indicates that increasing temperature increased the adsorption capacities of the reactive dyes. With increasing temperature from (30 to 50) °C, the values of q_m increased for RR-141 (5.0499 and 22.480, 7.713 and 13.592)

mg·g⁻¹ and RB-21 (16.548 and 70.028, 19.040 and 24.866) mg·g⁻¹ onto chitosan and APSP, respectively, indicating the endothermic nature of adsorption.

Table 1 compares the adsorption capacity of different types of adsorbents used for reactive dye adsorption. It is seen that the adsorbents used have comparable adsorption capacity to many of those reported in the literature.

Kinetics. To investigate the adsorption process of the dyes on APSP and chitosan, the pseudofirst-order, pseudosecond-order, and intraparticle diffusion models were used (eqs 3, 4, and 5; see Figure 5). Kinetic parameters are shown in Table 4. The rate of RR-141 and RB-21 adsorption by chitosan and APSP has been investigated under optimum pH and temperature using four different concentrations. The coefficients of determination were found to be higher for the second order (> 0.95) than the first order (> 0.81) for both RR-141 and RB-21 onto chitosan and APSP. The calculated q_e values increased with an increase in the initial dye concentration. The rate constants of both dyes varied over a wide range, suggesting that limiting steps may be chemisorption involving valency forces through the sharing and exchange of electrons between the sorbent and the substrate.⁴¹ The experimental data were also evaluated by the intraparticle diffusion kinetic model to investigate whether or not intraparticle diffusion is rate-limiting. According to the Weber–Morris model, a plot of uptake q_t versus the square root of time $t^{1/2}$ (figure not shown) should be linear if intraparticle diffusion is involved in the adsorption system, and if these lines pass through the origin, then the intraparticle diffusion is the rate-limiting step. The coefficients of determination R^2 for the intraparticle diffusion are not lower than that of the pseudosecond-order model (Table 4), and the plots do not pass through the origin, indicating some degree of boundary layer control and also that intraparticle diffusion is not the only rate-limiting step, but also other kinetic processes may control the rate of adsorption, all of which may be operating simultaneously.⁴²

FTIR. The IR spectra of PSP (palm shell powder), APSP, and chitosan are shown in Figure S1 of the Supporting Information. The strong broad band in the region of (3300 to 3500) cm⁻¹ is characteristic of the N–H stretching vibration although there is the possibility of overlapping between the N–H and the O–H stretching vibrations in chitosan. The absorption bands at (1630, 1590, 1381, 1080, and 1030) cm⁻¹ are ascribed to the C=O of amide I, NH, amide III, C₃–OH, and C₆–OH of chitosan, respectively. APSP showed a broad frequency at ~3419.42 cm⁻¹, which can be assigned to N–H/O–H stretching. The peak at ~1625.29 cm⁻¹ is characteristic of the N–H bond of amine or of the elongation of the aromatic –C=C– bonds. The peak at 1378.58 cm⁻¹ corresponds to C–N stretching, while the peak at 1200 cm⁻¹ is associated with the C–O stretching of the aromatic ring. PSP has peaks at (~1739 and ~1735) cm⁻¹ which shows the presence of carboxylic acid groups which is not seen in APSP. The characteristic peak of carbohydrates at ~1379 cm⁻¹ is seen in both PSP and APSP inferring the presence of lignin.

SEM. The morphology of PSP, APSP, and chitosan were studied using a scanning electron microscope (SEM) (Figure S2 of the Supporting Information). The surface of APSP was found to be irregularly rough and porous with identifiable micropores and mesopores in comparison to PSP. The SEM micrograph of chitosan shows that it has a larger number of pores connected by channels compared to APSP.

Brunauer–Emmett–Teller (BET) Analysis. The BET surface area of PSP, APSP, and chitosan was measured by nitrogen adsorption isotherms using a BET surface area analyzer (Mi-

croetrics ASAP 2020 V3.03H). The BET surface area was found to be (0.6735, 0.2979, and 1.11) m²·g⁻¹ for PSP, APSP, and chitosan, respectively.

Conclusion

APSP and chitosan were used as low-cost adsorbents for the removal of reactive red and reactive blue from aqueous solution. Equilibrium adsorption is achieved in about 60 min for APSP and 120 min for chitosan. The adsorption of the two dyes increase with an increase in temperature using both chitosan and APSP, suggesting that the process is endothermic. The results indicate that the data fit both the Freundlich model and Langmuir model for RR-141 and RB-21 onto APSP as well as chitosan. Kinetic data tended to fit the second-order kinetic model well. The reactive dyes are bound to chitosan through electrostatic attraction, between the anionic groups of the dyes and the protonated amine groups of the chitosan below the pK_a value of chitosan. Chitosan was found to have a higher adsorption capacity as compared to APSP. The study can be useful in the design of treatment plants for dye containing effluents.

Acknowledgment

The authors also thank Dr. P. K. Mehta, Department of Physics, for the XRD analysis and Dr. V. J. Rao, Department of Metallurgy and Material Science, for TGA and SEM analysis, and The M. S. University of Baroda and Head Department of Chemistry, The M. S. University of Baroda, for laboratory facilities.

Supporting Information Available:

FTIR spectra of PSP, APSP, and C in Figure S1 and scanning electron micrographs for PSP, APSP, and C in Figure S2. This material is available free of charge via the Internet at <http://pubs.acs.org>.

Literature Cited

- (1) Mittal, A. K. Studies on sorption of dyes by sulphonated coal and Garodama Cudium. *Ind. J. Environ. Health* **1989**, *3*, 105–111.
- (2) Judkins, J. F.; Hornsby, J. S. Color removal from textile dye waste using magnesium carbonate. *J. Water Pollut. Control Fed.* **1978**, *50*, 2446–2456.
- (3) Tan, L.; Sudak, R. G. Removing color from a groundwater source. *J. Am. Water Works Assoc.* **1992**, *84*, 79–87.
- (4) Al-Dege, Y.; Kharaishah, M. A. M.; Alen, S. J.; Ahmad, M. N. Effect of carbon surface chemistry on the removal of reactive dyes from textile effluent. *Water Res.* **2000**, *34*, 927–935.
- (5) Namasivayam, C.; Sumithra, S. Adsorption of Anionic Dyes on the Waste Fe(III)/Cr(III). *J. Environ. Sci. Eng.* **2006**, *48*, 69–74.
- (6) Namasivayam, C.; Dinesh, M. K.; Selvi, B. K.; Ashruggunissa, R.; Vasanthi, T.; Yamuna, R. T. Waste coir pith, a potential biomass for the treatment of dyeing waste water. *Biomass Bioenergy* **2001**, *21*, 477–483.
- (7) Gupta, V. K.; Suhas. Application of low cost adsorbent for dye removal - A review. *J. Environ. Manage.* **2009**, *90*, 2313–2342.
- (8) Gregorio, C. Non-conventional low cost adsorbent for dye removal: A review. *Biores. Technol.* **2006**, *97*, 1061–1085.
- (9) Dogan, K.; Akgul, E.; Sema, T.; Ferruh, E.; Mehmet, A. K.; Mustafa, T. Basic and reactive dye removal using natural and modified zeolites. *J. Chem. Eng. Data* **2007**, *52*, 2436–2441.
- (10) Namasivayam, C.; Yamuna, R. T. Removal of Congo red from aqueous solutions by biogas waste slurry. *J. Chem. Technol. Biotechnol.* **1992**, *53*, 153–7.
- (11) Thangamani, K. S.; Sathishkumar, M.; Sameena, Y.; Vennilamani, N.; Kardivelu, K.; Pattabhi, S.; Yun, S. E. Utilisation of modified silk cotton hull waste as an adsorbent for the removal of textile dye (reactive blue MR) from aqueous solution. *Biores. Technol.* **2007**, *98*, 1265–1269.
- (12) Sugunadevi, S. R.; Sathishkumar, M.; Shathi, K.; Kardivelu, K.; Pattabhi, S. Removal of direct T-blue R from aqueous solution onto carbonized sugarcane baggase waste. *Indian J. Environ. Protect.* **2002**, *22*, 500–505.

- (13) Namasivayam, C.; Yamuna, R. T. Colour removal from aqueous solutions by biogas residual slurry. *Toxicol. Environ. Chem.* **1993**, *38*, 131–43.
- (14) Namasivayam, C.; Yamuna, R. T. Utilizing biogas residual slurry for dye adsorption. *Am. Dyest. Rep.* **1993**, *83*, 22–8.
- (15) Tsai, W. T.; Chang, C. Y.; Lin, M. C.; Chien, S. F.; Sun, H. F.; Hsieh, M. F. Adsorption of acid dye onto activated carbons prepared from agricultural waste baggase by $ZnCl_2$ activation. *Chemosphere* **2001**, *45*, 51–58.
- (16) Namasivayam, C.; Kanchana, N.; Yamuna, R. T. Waste banana pith as adsorbent for removal of Rhodamine B from aqueous solutions. *Waste Manage.* **1993**, *13*, 89–95.
- (17) Mallik, P. K. Dye removal from waste water using activated carbon developed from sawdust; adsorption equilibrium and kinetics. *J. Hazard. Mater.* **2004**, *B113*, 81–88.
- (18) Morias, L. C.; Fretas, O. M.; Goncalves, E. P.; Vasconceles, L. T.; Gonzalez Beca, C. J. Reactive dyes removal from wastewaters by adsorption on eucalyptus bark: variables that define the process. *Water Res.* **1999**, *33*, 979–988.
- (19) Juang, R.; Wu, F.; Tseng, R. Mechanism of adsorption of dyes and phenols from water using activated carbons prepared from pulm kernels. *J. Colloid Interface Sci.* **2000**, *227*, 437–444.
- (20) Namasivayam, C.; Muniyasamy, N.; Gayathri, K.; Rani, M.; Ranganathan, K. Removal of dyes from aqueous solutions by cellulosic waste orange peel. *Bioresour. Technol.* **1996**, *57*, 37–43.
- (21) Knocke, W. R.; Homphil, L. H. Mercury(II) sorption by waste rubber. *Water Resour.* **1981**, *15*, 275.
- (22) Kumar, P.; Dara, S. S. Binding heavy metal ions with polymerized onion skin. *J. Polym. Sci.* **1981**, *19*, 397.
- (23) Raji, C.; Anirudhan, T. S. Removal of Hg(II) from aqueous solution by sorption on polymerized sawdust. *Ind. J. Chem. Technol.* **1996**, *3*, 49.
- (24) Navarvo, R. R.; Sumi, K.; Fugir, N.; Matsumuru, M. Mercury removal from waste water using porous cellulose camer modified with polyethylene amine. *Water Resour.* **1996**, *30*, 2488.
- (25) Sanchez, P. M.; Utriolla, R. Adsorbent-adsorbate interactions in the adsorption of Cd(II) and Hg(II) on ozonised activated carbons. *Environ. Sci. Technol.* **2002**, *36*, 3850–854.
- (26) Shan, H. Y.; Kay, G. M. Kinetic models for the sorption of dye from aqueous solution by wood. *Ind. Chem. Eng.* **1998**, *76B*, 183–191.
- (27) Choong, J. Mercury ion removal using a packed bed column with granular aminated chitosan. *J. Microbiol. Biotechnol.* **2005**, *15*, 497–501.
- (28) Lagergren, S. About the theory of so-called adsorption of soluble substances Kungliga Svenska Vetenskapsakademiens. *Handl. Band.* **1898**, *24*, 1–39.
- (29) Malik, P. K. Use of activated carbons prepared from saw dust and rice husk for adsorption of acid dyes: A case study of acid yellow 36. *Dyes Pigm.* **2003**, *56*, 239–249.
- (30) Namasivayam, C.; Kavitha, D. Removal of Congo red from water by adsorption onto activated carbon prepared from coir pith, an agricultural solid waste. *Dyes Pigm.* **2002**, *54*, 47–52.
- (31) Mohan, D.; Kunwar, P. S.; Gurdeep, S.; Kumar, K. Removal of Dyes from Wastewater Using Flyash, a Low-Cost Adsorbent. *Ind. Eng. Chem. Res.* **2002**, *41*, 3688–3695.
- (32) Sarkar, B.; Xi, Y.; Megharaj, M.; Krishnamurthy, S. R. G.; Naidu, R. Synthesis and characterisation of novel organopalygorskites for the removal of p-nitrophenol from aqueous solution: Isothermal studies. *J. Colloid Interface Sci.* **2010**, *350*, 295–304.
- (33) Freundlich, H. M. F. Uber die adsorption in lasugen. *Z. Phys. Chem. (Leipzig)* **1906**, *7*, 385–470.
- (34) Langmuir, I. The constitution and fundamental properties of solids and liquids. *J. Am. Chem. Soc.* **1916**, *38*, 2221–2295.
- (35) Bhatnagar, A.; Jain, A. K.; Mukul, M. K. Removal of Congo red from water using carbon slurry waste. *Environ. Chem. Lett.* **2005**, *2*, 199–202.
- (36) Netpradit, S.; Thiravetyan, P.; Towprayoon, S. Application of waste metal hydroxide sludge for adsorption of azo reactive dyes. *Water Res.* **2003**, *37*, 763–772.
- (37) Gwendolyn, G.; Tobin, J. M.; Guibal, E. Influence of Chitosan Preprotonation on Reactive on Black 5, sorption isotherms and Kinetics. *Ind. Eng. Chem. Res.* **2004**, *43*, 1–11.
- (38) Crini, G. Non-conventional low-cost adsorbents for dye removal: A review. *Bioresour. Technol.* **2006**, *97*, 1061–1085.
- (39) Ong, S. T.; Lee, C. K.; Zainal, Z. Removal of basic and Reactive dyes using ethylenediamine modified rice hull. *Bioresour. Technol.* **2007**, *98*, 2792–2799.
- (40) Hyun-Dock, C.; Min-Chul, C.; Do-Hyung, K.; Chil-Sung, J.; Kitae, B. Removal characteristics of reactive black 5 using surfactant-modified activated carbon. *Desalination* **2008**, *223*, 290–298.
- (41) Ho, Y. S.; Kay, G. M. Pseudo second order model for sorption processes. *Process Biochem.* **1999**, *34*, 451–465.
- (42) Weber, W. J.; Morris, J. C. Kinetics of adsorption on carbon from solution. *J. Sanit. Eng. Div., Am. Soc. Civ. Eng.* **1963**, *89*, 31–59.

Received for review July 9, 2010. Accepted November 12, 2010. The authors thank UGC-RFSMS for financial support.

JE1007263